Band structure and chemical bonding in $C_{58}BN$ heterofullerenes

Keivan Esfarjani, Kaoru Ohno, and Yoshiyuki Kawazoe
Institute for Materials Research, Tohoku University, 2-1-1 Katahira, Aoba-ku, Sendai 980, Japan
(Received 17 June 1994)

Using an all-electron mixed-basis approach and within the local-density approximation, the electronic structure of $C_{58}BN$ heterofullerenes in the solid fcc phase ($F\bar{3}m$) has been calculated. We study the two cases where the boron and nitrogen atoms are neighbors and where they are located far apart. The effect of this substitutional doping, which is expected to create acceptor and donor levels in the gap, is investigated and the electron dispersion relations are calculated in both cases. We find that when N and B are neighbors the donor and acceptor levels are pushed into the continuum, and we deduce that this configuration is slightly more stable than the one in which they are far apart. Total and partial charge densities of the occupied bands are displayed. From the present study, we have concluded that there is a single bond between N and B when they are neighbors, and the additional two electrons are mostly localized around N, and therefore only a small relaxation of the atoms is expected.

I. INTRODUCTION

The discovery of fullerenes as stable structures of carbon clusters[1,2] has stimulated much interest in the existence of similar type of clusters constructed with different species. For example, by laser vaporization supersonic cluster beam studies, Guo *et al.*[3] deduced that several carbon atoms in C_{60} were replaced by boron atoms, forming $C_{60-n}B_n$. Miyamoto *et al.*[4] calculated the electronic structure of hypothetical fcc $C_{59}B$ as a simple example, and found a metallic boron-induced acceptor state above the valence band. These newly proposed clusters are often called "heterofullerenes." They are different from the so-called endofullerenes[5] which have one or several different atoms (clusters) inside the cage. The discussion of their stability is still far from comprehensive. A cluster experiment even suggests a possibility of $B_{36}N_{24}$ with the same soccer-ball-shaped cage structure,[6] although no further confirmation has been reported yet.

The effect of doping was first studied in the context of superconductivity, but because of its semiconducting properties, we would like to investigate the effect of substitutional doping by nitrogen and boron atoms in C_{60} icosehedral fullerenes. Several band-structure calculations,[7] as well as experimental findings,[8] have revealed that the solid phase of C_{60} has a fcc structure with $Fm\bar{3}m$ symmetry. The distance between nearest neighbors is 10 Å, whereas the diameter of the balls is only 7 Å.[1] It is believed that the intermolecular interaction between the icosahedral fullerenes in the solid phase is of Van der Waals type, since they rotate isotropically above 260 K.[9] C_{60} is known to be a semiconductor having a gap of 1.6 eV (Ref. 10) (although another group[11] reports a value of 2.3 eV), thus it would be interesting to study the influence of substitutional doping in the density of states (DOS) of crystalline heterofullerenes, which could have the effect of enhancing the transport and/or optical properties of these systems. Previous studies of CBN heterofullerenes were performed by Liu, Gu, and Han[15] using the tight binding method.

Carbon has a graphite crystalline phase with layer stacking structure that stems from pure sp^2 hybridization. Boron nitride (BN) also has a stable graphitelike crystalline phase $H6$ with hexagonal sheets as well as a bct-1 phase. This hybridization is also present in C_{60} where each carbon atom has three neighbors that are connected to it by two single bonds and one double bond. If two carbon atoms of C_{60} associated with a double bond are replaced by a pair of boron and nitrogen atoms, in effect one has transported a proton from one nucleus to its neighbor. It would then be interesting to discuss the issue of charge transfer between the boron and the nitrogen sites; see Fig. 1. One could call the double bond the *covalent* limit, and the other extreme case where there is no bond between B and N but four additional electrons on N, the *ionic* limit. We call the intermediate case of a single N-B bond with two more electrons on N the *no charge transfer* limit. We could describe this limit with the image of an electron on N and a hole on B (compared to the average C_{60} medium), each of which would screen the excess charge of their corresponding nuclei. Therefore, the main theoretical interest lies in investigating the bonding character and the stability of this cluster as the simplest example of the carbon-boron-nitride heterofullerene. We can note that from an electrostatic point of view, the ionic limit is unrealistic since there cannot be more than two electrons on an ion that has only two more protons; the tendency to form a covalent bond between N and B is also against the creation of an ionic bond. We cannot however rule out the possibility of such a bonding, since it is present in ionic solids. For example in NaCl, Cl, the ion with the larger number of protons would attract one more electron to complete its shell and acquire a negative charge. The reason for this kind of transfer of charge is purely quantum mechanical. In general III-V elements are known to form polar bonds, whereas

0163-1829/94/50(24)/17830(7)/$06.00 ©1994 The American Physical Society

(a) The COVALENT LIMIT: Tendency to make a double bond by transfering one electron from N to B.

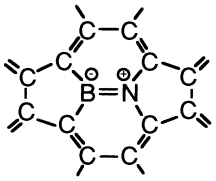

(b) The IONIC LIMIT: Tendency to make an ionic bond by transfering one electron from B to N.

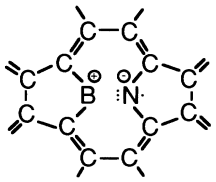

(c) Possibility of NO CHARGE TRANSFER; one excess electron at N site and one hole at B site (compared to the average C_{60} medium), each of which screens the excess charge of the nuclei of B and N.

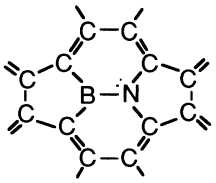

FIG. 1. Diagrams displaying the three different limits of chemical bonding between N and B.

I-VII elements form ionic bonds. So, there is generally competition between these effects, and the answer to the question of transfer of charge can be given if one uses a linear combination of atomic orbitals type of approach where the basis functions are only localized orbitals.

On the other hand, in the case where the N and B are located far apart, it would be of importance to study in particular the creation of new acceptor and donor levels in these materials.

As is well known from experimental data at room temperatures, the crystalline structure of solid C_{60} is fcc ($Fm\bar{3}m$) which results from their rapid isotropic rotation around their lattice site. In a band-structure calculation however, normally only one orientation can be adopted, and that lowers the symmetry of the space group. The density of states coming from such a calculation is obviously not identical to the experimental curve if one does not take care of the averaging associated with the rotations ideally needed in a band calculation. The importance of the orientation of the molecules within the unit cell has already been emphasized by several authors (see Refs. 7 and 12, for example). This orientation can affect largely the dispersion relation. In the $C_{58}BN$ case however, due to the presence of the N-B pair, a polarity could be induced in the molecule, and one expects that an ordering with a transition temperature higher than 260 K would occur. This would mean that at room temperatures the adopted $F\bar{3}m$ symmetry is more realistic than in the C_{60} case. In our study, since an accurate calculation of the total energy with an accuracy of less than 1 eV to determine the ground state is not possible at the moment, we only consider one of the most symmetric configurations for which the three axes pass through the center of the double bonds (see Fig. 2). Furthermore, we will also show the effect of the anisotropy of the cage on the dispersion relations, and see how this can induce a large variation in the energy bands.

In this paper, we present an *ab initio* calculation of $C_{58}BN$ with fcc crystal symmetry, by using our all-electron mixed-basis formalism. This method has already been applied to C_{60} and C_{70} layers[13] or crystals.[12] We have calculated the electronic structure of solid $C_{58}BN$ in the following two cases:

Case I (N and B neighbors): The molecule has the orientation shown in Fig. 2 where the N and B are neighbors. In this case, the B-N bond is parallel to the fcc [010] crystallographic axis and the center of this bond is on the [001] axis.

Case II (N and B apart): The molecule has the orientation shown in Fig. 2 where the N and B are images of each other after the inversion symmetry with respect to the center of the molecule. In this case again the three axes pass through the center of the double bonds, and the N and B are in the YZ plane.

We will also compare the above two cases to the electronic structure of solid C_{60} with the corresponding $Fm\bar{3}$ symmetry (where again each of the X, Y, and Z axes pass through the middle of a C=C double bond). The rest of this article is organized as follows: In Sec. II, we briefly review the mixed-basis formalism because this method is not commonly used by other authors. In Sec. III, we present our results and Sec. IV is devoted to concluding remarks.

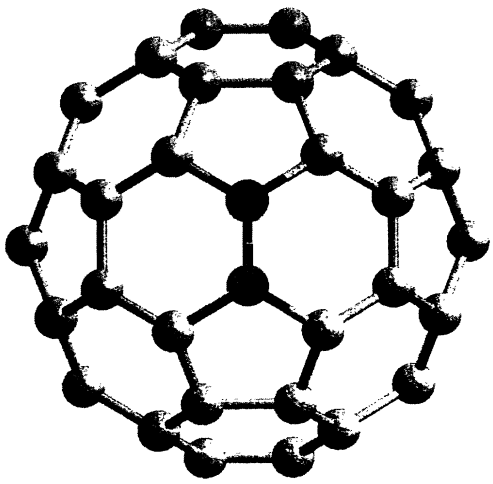

FIG. 2. Orientation of the $C_{58}BN$ molecule in the unit cell in case I where B and N are neighbors. The Z axis is directed upwards perpendicular to the plane of the figure. The N-B bond is along the Y direction. This is an orthographic projection on the XY plane. In case II, we adopt the exact same structure except that the blue atom is switched with its mirror image with respect to the XY plane.

II. ALL-ELECTRON MIXED-BASIS FORMALISM

We use a self-consistent all-electron mixed-basis approach within the local-density approximation. The mixed-basis method was first introduced by Louie *et al.*[14] in order to treat the d orbitals of transition metals within the pseudopotential formalism. A combined set of plane waves (PW's) and Bloch sums of atomic orbitals (AO's) is used as basis functions. That enables us to represent both the highly localized and the extended character of the electronic wave functions. Recently, we[13,12] developed the mixed-basis method by including not only valence but also core electrons in order to deal with two- and three-dimensional C_{60} crystals. This method turns out to be quite efficient for lighter elements such as the first two rows of the Periodic Table.

For each $\mathbf{k}$ in the Brillouin zone, the basis set $|l\rangle$ is either the PW

$$\frac{1}{\sqrt{\Omega}} e^{i(\mathbf{k}+\mathbf{G})\cdot\mathbf{r}} \tag{1}$$

or the AO which is of the Bloch form

$$\Phi_{i\mu}(\mathbf{k},\mathbf{r}) = \frac{1}{\sqrt{\Omega}} \sum_{\mathbf{R}_m} e^{i\mathbf{k}\cdot(\mathbf{R}_m+\tau_i)} f_{i\mu}(\mathbf{r}-\mathbf{R}_m-\tau_i). \tag{2}$$

Here $\mathbf{G}$ is a reciprocal-lattice vector, $\mathbf{R}$ a primitive vector, μ a label for the orbitals on the ith atom: τ_i represents the position of atom i within the unit cell, and Ω the volume of the crystal. In our formulation, we use Slater-type orbitals for $f_{i\mu}$, which are, in the present calculation, $1s$, $2p_x$, $2p_y$, and $2p_z$ for each atom. We found that due to their extended character, the $2s$ Slater orbitals were well represented with plane waves of relatively large wavelength; furthermore, since they are not orthogonal to the $1s$ states additional numerical complications arise in the Choleski decomposition of the overlap matrix. We, therefore, did not include them in our basis functions.

Since the basis functions are not orthogonal to each other, the orthogonalization procedure is necessary in the calculation. For this purpose, we introduce the overlap matrix $S = \{\langle k|l\rangle\}$, and use the Choleski decomposition of the form: $S = UU^{\dagger}$ with U being a lower half triangular matrix.[14]

The effective one-electron Hamiltonian has the general form $H = T + V$ with $T = -\frac{1}{2}\nabla^2$ as the kinetic energy (we use the atomic units in which $\hbar = m = e = 1$, 1 a.u. = 0.529 Å and 1 a.u. = 27.2 eV = 2 Ry) and

$$V(\mathbf{r}) = -\sum_n \frac{Z_n}{|\mathbf{r}-\mathbf{R}_n|} + \int d\mathbf{r}' \frac{\rho(\mathbf{r}')}{|\mathbf{r}-\mathbf{r}'|} + V^{\mathrm{xc}}(\mathbf{r}) \tag{3}$$

as the potential energy. Here $V^{\mathrm{xc}}(\mathbf{r})$ is a local exchange-correlation potential which is evaluated in real space under the local-density approximation. In the $X\alpha$ method, it is given by

$$V^{\mathrm{xc}}(\mathbf{r}) = -3\alpha\left(\frac{3}{8\pi}\rho(\mathbf{r})\right)^{1/3}. \tag{4}$$

We used this form of the exchange-correlation potential with $\alpha = 0.9$.

The integrations over the unit cell are done in the real space. The kinetic energy as well as part of the potential matrix element calculations are done analytically: to take care of the divergence at the center of the nuclei, we write the potential as

$$V(\mathbf{r}-\mathbf{R}) = \frac{e^{-\zeta|\mathbf{r}-\mathbf{R}|}}{|\mathbf{r}-\mathbf{R}|} + V_{\mathrm{rest}}(\mathbf{r}).$$

The first term can be handled analytically, and if the parameters ζ corresponding to each element are properly chosen, it can include more than 90% of the whole value of the matrix element. The second term V_{rest} is integrated numerically on a $64 \times 64 \times 64$ grid. The fast Fourier transforms are also computed using this grid. We set the damping parameters α_{1s} and α_{2p} of the Slater type AO's, so as not to overlap with those at neighboring atomic positions. The numerical values of these parameters are displayed in Table I. For the coordinates of the atoms, we assumed the truncated icosahedron structure that is exactly the same as C_{60}. We chose 1.46 Å for the length of single bonds and 1.40 Å for the lengths of double bonds. The lattice constant a was taken to be the same as 10.42 Å of the usual C_{60} fcc.

Since the Brillouin zone is small, we "integrate" over only the Γ point to get the total electron density.

Our basis functions consisted of 2109 plane waves, and 60×4 Slater $1s, 2p_x, 2p_y$, and $2p_z$ orbitals.

III. RESULTS FOR THE ELECTRONIC STRUCTURE OF SOLID $C_{58}BN$

Since C_{60} can exothermically solidify with an fcc crystalline structure, we expect that $C_{58}BN$ can also solidify with a fcc lattice, since it has a closed shell structure.

Due to the much less symmetrical form of the $C_{58}BN$ molecule, the irreducible Brillouin zone (BZ) is a quarter of the whole zone, which is twelve times bigger than the usual 1/48 irreducible BZ. In particular, from the dispersion relations of Figs. 3 and 4, we can see that several degenerate levels at symmetry points are split into nondegenerate single levels because of the lower symmetry (C_3 around [111] is broken for example).

For simplicity, we just compare the dispersion curves of C_{60} and $C_{58}BN$ inside a 1/48 BZ; see Figs. 3, 4, and 5, respectively, for $C_{58}BN$ and C_{60}, remembering that the point denoted by Z represents the $\langle 001\rangle$ direction, i.e., toward the location of the impurity, because it is not equivalent to the Y $\langle 010\rangle$ or X $\langle 100\rangle$ point, for ex-

TABLE I. Damping parameters of the atomic orbitals and the ionic potential in atomic units.

Parameter	C	B	N
$1/\alpha_{1s}$	0.18	0.21	0.15
$1/\alpha_{2p}$	0.21	0.25	0.20
$1/\zeta$	0.7	0.8	0.6

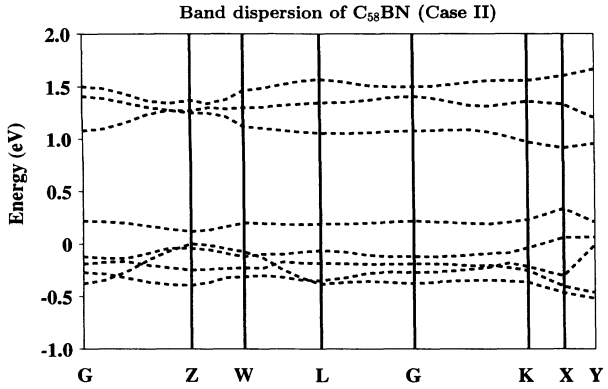

FIG. 3. Band dispersion of $C_{58}BN$ in case II. The donor and acceptor levels can easily be identified. To show the effect of the anisotropy of the cage, we have also displayed the energies of the $X\langle 100\rangle$ and $Y\langle 010\rangle$ points besides the $\langle 001\rangle$ point denoted by Z. The K and W points are respectively along the $\langle 011\rangle$ and $\langle 012\rangle$ directions. The electron seems lighter than the hole in the considered Z direction. G is of course the Γ point.

ample. The energies at the latter symmetry points are unchanged for C_{60}, but are different in the case of $C_{58}BN$. To illustrate this change, we show their values near the K point in the above figures.

In case I, where the N and B are neighbors, we found that there is no donor or acceptor level in the band gap, as was in the $C_{59}B$ case.[4] Furthermore, the bands, except for a broadening, and splitting of degenerate levels, seem quite similar to the C_{60} case. In case II where N and B are far apart however, the expected donor and acceptor levels are present; there is a large anisotropy in the bands along X, Y, and especially the Z directions, and the bands seem generally flat. The band structure of the two cases do not look very similar, but after a closer examination, one can notice that the donor band of case II is just the third conduction band of case I shifted *down* by about 0.5 eV. This, by the way, causes an accidental degeneracy near the Z point. The same holds for

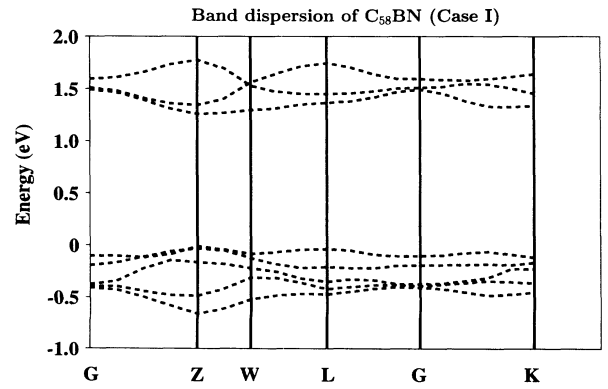

FIG. 4. Band dispersion of $C_{58}BN$ in case I. The donor and acceptor levels have entered the continuum due to their strong hybridization. The point denoted by Z is in the $\langle 001\rangle$ direction; the X and Y points have not been displayed here.

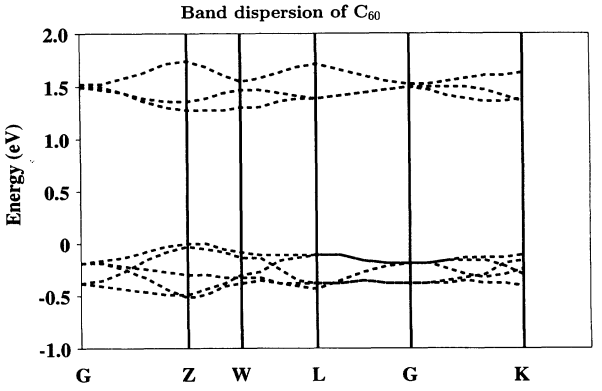

FIG. 5. Band dispersion of C_{60}. In this figure, as well as the Figs. 3 and 4, the coordinates of the considered K points in units of $2\pi/a$ are $G(0,0,0) \rightarrow Z(0,0,1) \rightarrow W(0,1/2,1) \rightarrow L(1/2,1/2,1/2) \rightarrow G(0,0,0) \rightarrow K(0,3/4,3/4) \rightarrow X(1,0,0) \rightarrow Y(0,1,0)$.

the acceptor level of case II which is the lowest valence band of case I shifted *up* by about 0.7 eV. The rest of the bands are quite similar in shape and energy. According to Ref. 4, there should be an acceptor, as well as a donor level, due to boron and nitrogen, in the gap. However, since in case I the two atoms are close, there would be a large coupling between them. So, considering the above remark on the calculated dispersion curves, we interpret this absence of donor and acceptor levels in case I, in terms of strong coupling and hybridization between these two levels that pushes them into the valence and conduction bands.

Regarding the stability of the two cases, we argue that case I has lower energy because the mentioned hybridization pushes the valence levels to lower, and the conduction levels to higher, energies. Since only the valence levels are occupied, the energy of case I, when the coupling is strongest, is lower. One can also argue from an

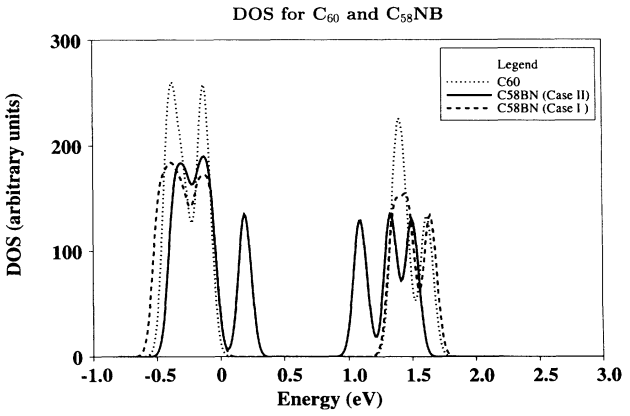

FIG. 6. Density of states of $C_{58}BN$ in case II (solid line) compared to C_{60} (dotted line). Only the three conduction and the five valence bands around the gap have been displayed. The broadening was obtained by convolution with a Gaussian of width 0.05 eV. The DOS in case I is indicated with the dashed line; it is quite similar to C_{60} except for a broadening.

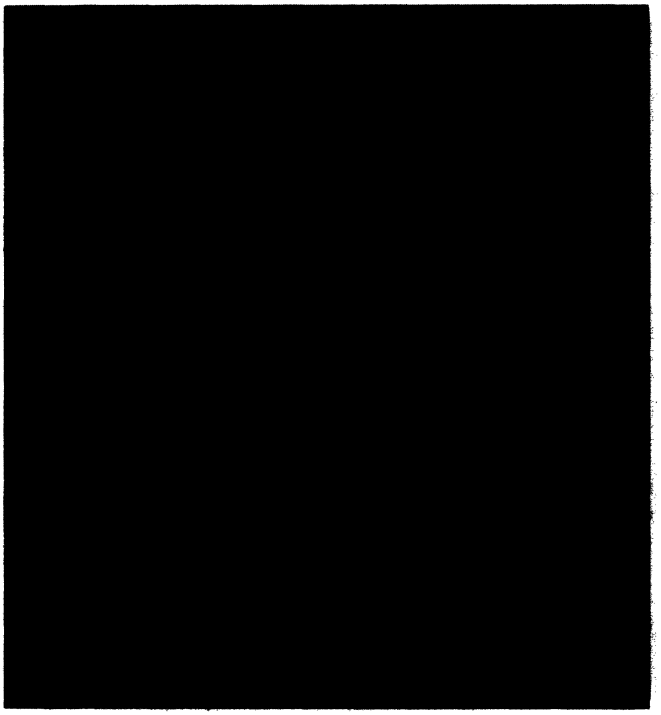

FIG. 7. Isosurfaces of the partial charge density of the five highest valence bands of $C_{58}BN$ in case I. The corresponding partial charge of C_{60} has been subtracted. The X axis is perpendicular to the plane of the figure. One can clearly see on the left the hole state (the larger blue area) around B in this case. The warmer colors represent regions of negative density (electron) and the colder colors regions of positive density (hole).

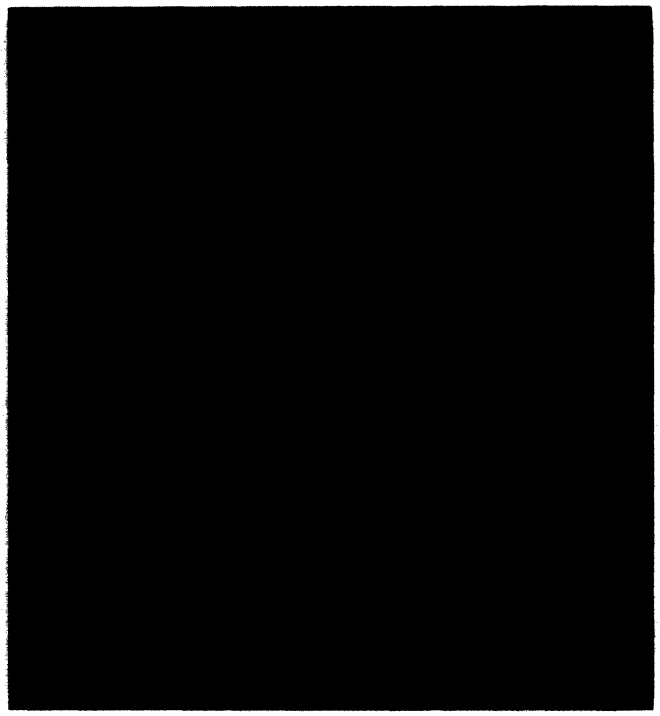

FIG. 8. Total charge density of the $C_{58}BN$ in case I. Displayed are three surfaces of constant density of values 0.005, 0.008, and 0.02, respectively. (The total electronic charge in the $64 \times 64 \times 64$ grid is normalized to 360.) One can differentiate the double bonds between two hexagons from the single bonds. To avoid superposition with the density from the back of the molecule, a part of the latter has been cut by a dark inclined plane.

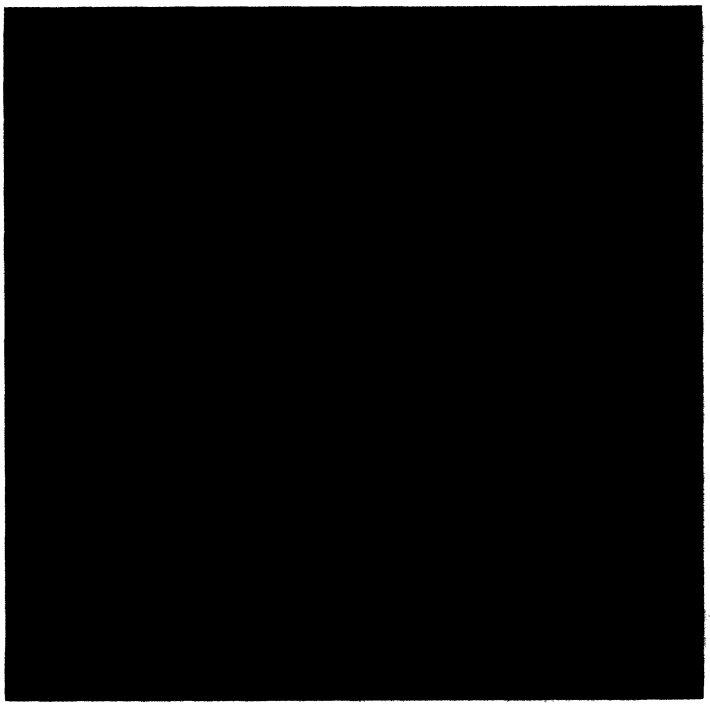

FIG. 9. Total charge density of the $C_{58}BN$ in case I from which the density of C_{60} has been subtracted. Displayed are four surfaces of constant density of values ± 0.005 and ± 0.001, respectively. Warm colors represent electron excess, and cold colors a lack of it. We obtain very similar pictures for case II.

electrostatic point of view that since the boron and the nitrogen have slight charges of opposite signs in case I, the energy of the cluster would be lowest if N and B are close to each other, whereas if they are separated, the slight charge difference has a higher separation and thus a higher electrostatic energy.

Figure 6 shows the calculated DOS near the band gap in cases I and II. As we can see from their dispersion relation in Fig. 4, there is no special feature in the DOS of case I except for a slightly wider bands. For comparison, the DOS of C_{60} is shown in the same figure with dotted lines. The widths of the valence and the conduction bands are slightly larger in $C_{58}BN$ compared with C_{60}. This is expected since the introduction of the impurities always has the effect of broadening the bands. We must add that the displayed DOS is obtained from an interpolation of the bands in a small portion of the first Brillouin zone; the energy values have been broadened by convoluting them with a Gaussian of width 0.05 eV.

We have shown in Fig. 7 the partial charge density of the top five valence bands from which we have subtracted the corresponding charge density of C_{60}. One can clearly see the hole state in blue at the location of the boron atom. Furthermore, we can notice the π character of these five bands. The total charge being of course zero, we see equal areas of positive and negative charges. We find in particular that the charge distribution is mostly localized around the belt containing the N-B pair, that is the YZ plane which is also the plane of the figure. This is one signature of the anisotropy of the bands, i.e., there is no change as far as the $X(1,0,0)$ direction is concerned, but the Y and especially the Z directions are greatly affected by the B and N substitution.

Next, we present the resulting total charge density of $C_{58}BN$ (case I) in Fig. 8: There is an excess charge distribution around nitrogen, while there is a depletion of charge around boron. All the other features of the distribution seem the same as C_{60}. One can also differentiate the double bonds from the single C-C bonds. In analyzing these figures, one should keep in mind that these isosurfaces do not represent the orbitals, they are only surfaces of constant density, and their shape depends on the considered density value. For more clarity, we have also subtracted the total electron density of C_{60} from $C_{58}BN$, and we can, therefore, look at the isodensity surfaces for the electron-hole pair in Fig. 9. One may notice the following points:

(1) The two isodensity surfaces of the electron and the hole are not quite identical, more specifically, the two isosurfaces are further apart for the hole than for the electron. This suggests that the electronic wave function might be more delocalized and, therefore, that its effective mass is less than the hole. A look at the curvature at the Γ point of the dispersion relation of case II will confirm the above. Even though we do not have the same evidence for case I, we can compare the isodensity surfaces in both cases and come to the same conclusion.

(2) From our calculation, the net dipole moment per unit cell is zero in both cases with a rather good accuracy. In order to investigate on the nature of the chemical bonding, we calculated the difference in the charge between the nitrogen and the boron by counting the charge within a sphere of same radius around N and B. We found that in both cases I and II, the difference reaches a maximum of 1.8 ± 0.2 (see Fig. 10) as a function of the chosen radius. There is no easy way in our formalism to calculate the charge pertaining to an atom since our basis functions contain plane waves as well as atomic orbitals. However, we can, for the purpose of graphical representation, store the total charge density in the unit cell on a regular grid ($64 \times 64 \times 64$): that is how we arrived at the above number. The large uncertainty is due to the fact that the density is represented by discrete points in space, and depending on whether a point falls inside or outside the sphere of a given radius, there could be a big fluctuation in the counted charge. This result however was obtained assuming the same atomic volume for both N and B, which could be unrealistic. Clearly, the atomic volume of the nitrogen is larger than boron, and as a result, the charge difference could become slightly larger had we taken a larger radius for the nitrogen. For this reason, we cannot make an accurate statement regarding the amount of charge transfer, but it is certainly very near two. We, therefore, suspect that we are in the "*no charge transfer*" limit (see Fig. 1) where the bonding is neither covalent nor ionic, but just what we would call "polar." In this case the charge of the ions are screened and, therefore, there is almost no additional (compared to C_{60}) electrostatic interaction between N and B. Any slight deviation of the charge difference from the number 2 would result in an attractive interaction between the two atoms and thus a slightly smaller bond length. In addition to this displacement, we suspect that due to its larger atomic size, the nitrogen would be pushed slightly toward the boron, which in turn would move also in the same direction. Quantum molecular dynamic simulations to investigate the new relaxed positions are under way.

We noticed that when N and B were separated, there was a slightly smaller charge difference between N and B. This can be explained by using the fact that B being less electronegative than C, will give out its electron to N more easily than to C. Therefore, the charge difference between N and B would be larger if these two were

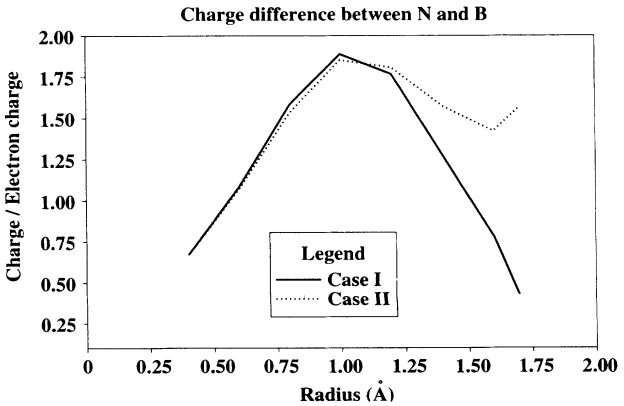

FIG. 10. Charge difference between N and B in both cases I and II. The error bars are not displayed but there is a 0.2 uncertainty for these values.

neighbors.

(3) Due to the presence of the donor and acceptor elements, a large anisotropy can be noticed in the bands. This effect is visible, for example, in Fig. 3 where we have displayed the three very different energy values at the $X\langle 100\rangle$, $Y\langle 010\rangle$, and $Z\langle 001\rangle$ points. This is of course due to the loss of C_3 symmetry around the $\langle 111\rangle$ direction. The important fact is the large difference in the three energy values which causes a much *wider band* in addition to the effect of orientation of the molecules already pointed out.[12]

IV. CONCLUSION

In this report, using an all-electron mixed-basis calculation, we showed the electronic structure of the fcc heterofullerene $C_{58}BN$. The nonexistence of any donor or acceptor levels in case I where N and B are neighbors was explained by a hybridization of these two levels resulting in their disappearance into the continuum. We were able to identify these two levels in the band structure of case II, and observed their shifts into the valence and conduction bands in case I. As a result, it was deduced that case I has lower energy, and, therefore, is slightly more stable. We also found that due to the electronegativity of nitrogen, there is almost one electron bound to it and almost a hole bound to the boron; and, therefore, the bonding has a strongly *polar* character, and this effect could result in a very slight relaxation of the N and B atoms toward each other in case I (if the charge difference is different from two), in addition to an eventual slight shift of the pair in the N to B direction due to the difference in the size of the atoms. In the present work, we fixed *a priori* the B-N bond length 1.40 Å, and we assumed the N and B occupy the position of carbons of the C_{60}; although further calculations of relaxing the bond length are highly desirable. We are now planning to perform an *ab initio* simulated annealing calculation within the all-electron mixed-basis formalism. And finally, we should emphasize on the importance of the anisotropy of the isoenergy surfaces that also results in a larger bandwidth.

ACKNOWLEDGMENTS

We are very grateful to the members of the computer science group of IMR for valuable discussions and also assistance in using computers. We also wish to thank Dr. Marcel Sluiter and Professor Koichi Shindo for the fruitful discussions, and Professor Bing Lin Gu for suggesting the problem. This work was partially supported by the Grant-in-Aid for Science Research on Priority Areas "Carbon Microclusters" from the Ministry of Education, Science and Culture of Japan.

[1] J. H Weaver and D. M. Poirier, Solid State Phys. **48**, 1 (1994), and references therein.
[2] R. F. Curl and R. E. Smalley, Science **242**, 1017 (1988); H. W. Kroto *et al.*, Nature **318**, 162 (1991).
[3] T. Guo, C. Jin, and R. E. Smalley, J. Phys. Chem. **95**, 4948 (1991).
[4] Y. Miyamoto, N. Hamada, A. Oshiyama, and S. Saito, Phys. Rev. B **46**, 1749 (1992).
[5] R. D. Johnson *et al.*, Nature **355**, 239 (1992); H. Shinohara *et al.*, *ibid.* **357**, 52 (1992).
[6] S. J. L. Placa *et al.*, Chem. Phys. Lett. **190**, 163 (1992).
[7] S. Saito and A. Oshiyama, Phys. Rev. Lett. **66**, 2637 (1991); N. Troullier and J. L. Martins, Phys. Rev. B **46**, 1754 (1992).
[8] R. M. Fleming *et al.*, in *Clusters and Cluster-Assembled Materials*, edited by R. S. Averback, J. Bernholc, and D. L. Nelson, MRS Symposia Proceedings No. 206 (Materials Research Society, Pittsburgh, 1991), p. 691.
[9] P. A. Heiney, J. Phys. Chem. Solids **53**, 1333 (1992).
[10] T. R. Ohno, Y. Chen, S. E. Harvey, G. H. Kroll, J. H. Weaver, R. E. Haufler, and R. E. Smalley, Phys. Rev. B **44**, 13 747 (1991).
[11] R. W. Lof *et al.*, Phys. Rev. Lett. **68**, 3924 (1992).
[12] B.-L. Gu, Y. Maruyama, J.-Z. Yu, K. Ohno, and Y. Kawazoe, Phys. Rev. B **49**, 16 202 (1994).
[13] Y. Kawazoe, H. Kamiyama, Y. Maruyama, and K. Ohno, Jpn. J. Appl. Phys. **32**, 1433 (1993); T. Hashizume *et al.*, Phys. Rev. Lett. **71**, 2959 (1993).
[14] S. G. Louie, K.-M. Ho, and M. L. Cohen, Phys. Rev. B **19**, 1774 (1979).
[15] J. N. Liu, B. L. Gu, and R. S. Han, Solid State Commun. **84**, 807 (1992).

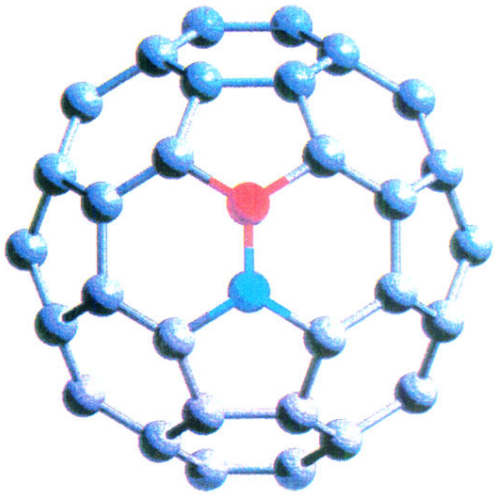

FIG. 2. Orientation of the $C_{58}BN$ molecule in the unit cell in case I where B and N are neighbors. The Z axis is directed upwards perpendicular to the plane of the figure. The N-B bond is along the Y direction. This is an orthographic projection on the XY plane. In case II, we adopt the exact same structure except that the blue atom is switched with its mirror image with respect to the XY plane.

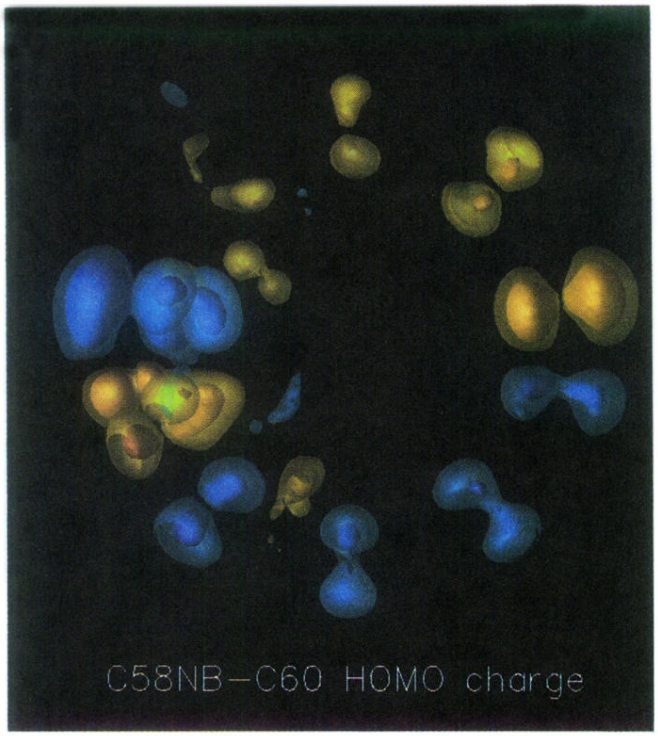

FIG. 7. Isosurfaces of the partial charge density of the five highest valence bands of $C_{58}BN$ in case I. The corresponding partial charge of C_{60} has been subtracted. The X axis is perpendicular to the plane of the figure. One can clearly see on the left the hole state (the larger blue area) around B in this case. The warmer colors represent regions of negative density (electron) and the colder colors regions of positive density (hole).

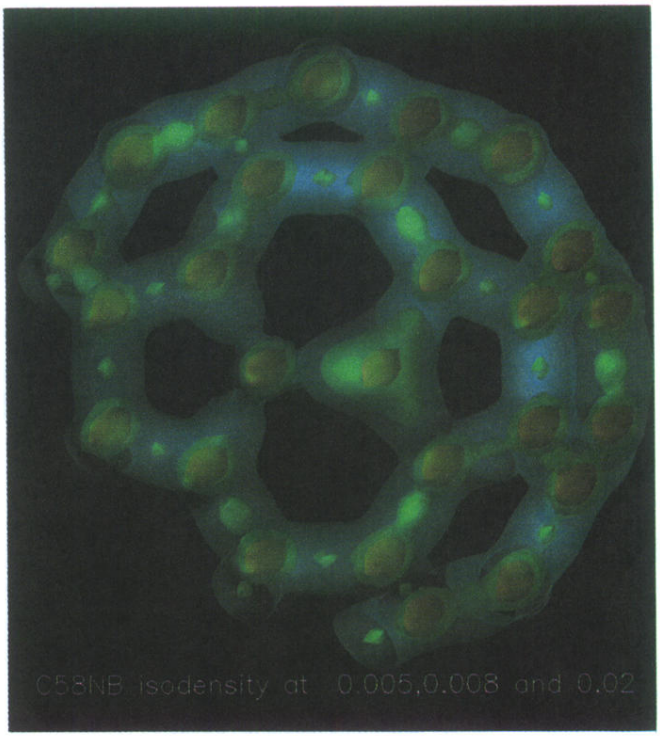

FIG. 8. Total charge density of the $C_{58}BN$ in case I. Displayed are three surfaces of constant density of values 0.005, 0.008, and 0.02, respectively. (The total electronic charge in the $64 \times 64 \times 64$ grid is normalized to 360.) One can differentiate the double bonds between two hexagons from the single bonds. To avoid superposition with the density from the back of the molecule, a part of the latter has been cut by a dark inclined plane.

FIG. 9. Total charge density of the $C_{58}BN$ in case I from which the density of C_{60} has been subtracted. Displayed are four surfaces of constant density of values ± 0.005 and ± 0.001, respectively. Warm colors represent electron excess, and cold colors a lack of it. We obtain very similar pictures for case II.